NRL/MR/4790—92-6984

Numerical Simulation of the Electromagnetic Instability of an Intense Beam in a Quadrupole Focusing System

J. KRALL, C. M. TANG, AND T. SWYDEN*

Beam Physics Branch
Plasma Physics Division

*FM Technologies, Inc.
Fairfax, VA

June 15, 1992

92

REPORT DOCUMENTATION PAGE

Form Approved
OMB No. 0704-0188

1. AGENCY USE ONLY (Leave blank)	2. REPORT DATE	3. REPORT TYPE AND DATES COVERED
	June 15, 1992	Interim

4. TITLE AND SUBTITLE

Numerical Simulation of the Electromagnetic Instability of an Intense Beam in a Quadrupole Focusing System

5. FUNDING NUMBERS

ARPA Order 7781

6. AUTHOR(S)

J. Krall, C. M. Tang, and T. Swyden*

7. PERFORMING ORGANIZATION NAME(S) AND ADDRESS(ES)

Naval Research Laboratory
Washington, DC 20375-5000

8. PERFORMING ORGANIZATION REPORT NUMBER

NRL/MR/4790--92-6984

9. SPONSORING/MONITORING AGENCY NAME(S) AND ADDRESS(ES)

DARPA
Arlington, VA 22203

NSWC
Silver Spring, MD 20903

ONR
Arlington, VA 22217

10. SPONSORING/MONITORING AGENCY REPORT NUMBER

11. SUPPLEMENTARY NOTES

*Technologies, Inc., Fairfax, VA

12a. DISTRIBUTION/AVAILABILITY STATEMENT

Approved for publication; distribution unlimited.

12b. DISTRIBUTION CODE

13. ABSTRACT *(Maximum 200 words)*

Discrete quadrupole focusing systems are subject to an electromagnetic instability wherein the growing transverse motion of the beam interacts with the quadrupole field and the TE_{11} waveguide mode. We study this via three-dimensional particle simulation. We find evidence of the instability, with growth rates and frequencies in reasonable agreement with theory. The instability is found to saturate at a low amplitude, however, and has no discernable effect on the macroscopic properties of the beam.

14. SUBJECT TERMS

Intense beam
Quadrupole focusing
Three-wave instability

15. NUMBER OF PAGES

18

16. PRICE CODE

17. SECURITY CLASSIFICATION OF REPORT	18. SECURITY CLASSIFICATION OF THIS PAGE	19. SECURITY CLASSIFICATION OF ABSTRACT	20. LIMITATION OF ABSTRACT
UNCLASSIFIED	UNCLASSIFIED	UNCLASSIFIED	SAR

CONTENTS

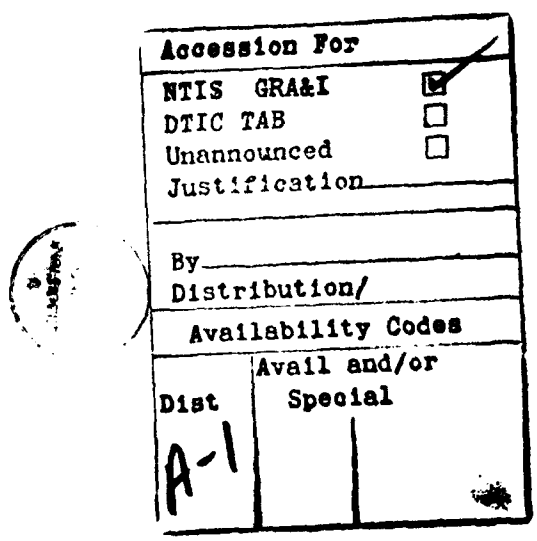

Numerical Simulation of the Electromagnetic Instability of an Intense Beam in a Quadrupole Focusing System

I. Introduction

Discrete quadrupole focusing systems, also called FODO lattices (for focusing field, zero field, defocusing field, zero field), have been used to transport charged particle beams for a variety of applications. A FODO lattice is an alternative to helical quadrupole windings for strong focusing. Helical quadrupole (stellarator) focusing systems have been found to be subject to an electromagnetic instability, which we referred to as the three-wave instability.[1-3] In the helical quadrupole case, the instability can be extremely disruptive to beam transport. This has been observed in numerical simulations[1,3] and in experiments.[4]

Here, we consider the corresponding instability for transverse perturbations of an electron beam interacting with a FODO lattice field and a TE_{11} waveguide mode. Specifically, we consider an alternating gradient quadrupole field (B_{qx}, B_{qy}), where

$$B_{qx} = -B_q k_q cos(nk_q z)y, \qquad B_{qy} = -B_q k_q cos(nk_q z)x, \qquad (1a-b)$$

$B_q k_q$ is the peak field gradient, $k_q = 2\pi/\lambda_q$ and λ_q is the period of the quadrupole field. This configuration has been studied theoretically[5,6] and, unlike the helical quadrupole case, a useful stable regime does not appear to exist.[5] Our present numerical study was motivated by the apparent need to discover a detuning mechanism for this instability, perhaps analogous to that found in Ref. 3 for the helical quadrupole configuration.

In Ref. 5, the dispersion relation for the instability was derived and numerical solutions were presented. These were shown to be in good agreement with approximate analytical expressions for the spatial and temporal growth rates. It was also shown that for given parameters, peak growth rates occur at a single frequency but with multiple wave numbers. Futhermore, it was found that secondary modes also exist, with multiple wave numbers at

Manuscript approved April 16, 1992.

each frequency. Numerical solutions to the dispersion relation show that these secondary modes have significantly lower growth rates than the primary mode. Finally, it was shown that the primary mode is "cut-off" when

$$\frac{k_q}{2} + \frac{1}{2}\sqrt{k_q^2 - 2k_q K_q} < \sqrt{\frac{\mu_{11}^2}{\gamma^2 - 1}}, \tag{2}$$

where $K_q = \Omega_q / v_b, \Omega_q = eB_q/\gamma m_e c$, v_b is the beam velocity, $\gamma = (1 - v_b^2/c^2)^{1/2}, e$ is the elementary charge (assumed positive), m_e is the electron mass, c is the speed of light, $\mu_{11} r_g$ is the first postive zero of the Bessel function J_1', r_g is the radius of the waveguide through which the beam is being transported, and ' indicates a derivative of J_1 with respect to its argument.

As an example, an (ω, k) diagram is given in Fig. 1 for a case in which the quadrupole gradient is $B_q k_q = 1000$ G/cm, the wave number is $k_q = 0.55$ cm^{-1}, the waveguide radius $r_g = 3$ cm and $\gamma = 7$. For clarity, the diagram corresponds to the limit of zero beam current. In Fig. 1, the primary mode occurs at points indicated by a circle. Secondary modes occur where an unstable beam mode (straight line) intersects a waveguide mode (curved line) other than the primary mode. These are indicated by squares. Figure 2 shows the temporal growth rate of the primary instability, $Im(\omega/c)$ plotted versus wave number for the parameters of Fig. 1, but with beam current $I_b = 2$ kA. These figures, which are obtained by numerically solving Eq. (23) of Ref. 5, show the periodic nature of the instability.

II. Numerical Results

Simulations were performed using the ELBA[7] code. ELBA is a three-dimensional particle code which simulates a beam propagating within a cylindrical metallic pipe. The full set of Maxwell's equations along with the full relativistic motion of the beam particles are included. The ELBA code contains numerous beam diagnostics, including an rms emittance diagnostic[8] that was developed for beams with x-y coupling.

For each simulation, initial particle positions and velocities were "matched" to the FODO field in the envelope sense as in Ref. 9, including an ad hoc correction for space charge. For comparison to the ELBA runs, simulations were also performed using the SST[10] code. The SST code is a single-slice version of the ELBA code which is valid in the limit that the beam radius is small compared to the length scales of the beam and the external fields in the axial direction. Because the derivatives versus the axial direction are dropped in this approximation, the SST code cannot exhibit the instability. This allowed us to distinguish physical effects (current loss, emittance growth, etc.) that may be caused by the instability from those that arise from imperfections in the matching scheme (see, e.g., Ref. 11).

Growth rates were measured by analyzing the TE_{11} mode, for which the B_z and E_r components may be "projected out" from the electromagnetic spectrum in a straightforward manner. The growth rate is then obtained as a function of ω and k for those cases in which an unstable mode grew above the background "noise". Because our simulation takes place in a coordinate system that moves with the beam $(r, \theta, \zeta = ct - z)$, these growth rates are $\Gamma/c = Im(\omega/c - k)$. This corresponds to the theoretical result only in the case that $Im(k) = 0$ as was assumed in numerically solving the dispersion relation.

Simulations were performed for parameters typical of a high-current, induction accelerator beam, $I_b = 1 - 2$ kA, $\gamma_o = 7$ and normalized rms emittance, $\epsilon_{n,rms} = 0.05 - 0.16$ cm-rad. Simulation parameters are listed in Table I. In a typical run, a beam of length $L_b = 250$ cm was transported over 10 meters in the presence of the external focusing fields. It was not practical to simulate a case in which the primary mode is "cut-off," as given by Eq. (2). For the parameters of Fig. 2, for instance, this would require either $\gamma < 1.4$ or

$r_g < 0.43$ cm.

In each run, we found a growing TE_{11} mode as predicted by theory, but without a growing displacement of the beam centroid. In fact, the instability saturated at a low level, apparently due to mode competition between the various wave numbers and, possibly, between the primary and secondary modes.

As an example, we return to the parameters of Fig. 2. Here, we simulated an $L_b =$ 250 cm, $I_b = 2$ kA, $\gamma = 7, \epsilon_{n,rms} = 0.05$ cm-rad beam propagating for 10 meters. The following was observed:

1) As the TE_{11} mode grew, the peak frequency of the spectrum shifted continuously. Exponential growth rates could only be obtained by plotting the log of the peak of the Fourier transform of the TE_{11} mode versus propagation distance z, as in Fig. 3. The points in Fig. 3 show approximately linear growth over the first 300 cm of propagation with growth rate $\Gamma/c = 0.023$ cm^{-1} and frequency $\omega/c = 0.58 \pm 0.12$ cm^{-1}. Theoretical values for this case are $\Gamma/c = 0.024$ cm^{-1} and frequency $\omega/c = 0.67 \pm 0.04$ cm^{-1}, where we are quoting the half-width at half-maximum of the Γ/c versus ω/c curve as the expected frequency spread.

2) Early in the simulation the wave number spectrum, shown in Fig. 4, resembled that expected from Fig. 2. At later times the spectrum is broadband. This is shown in Fig. 5.

3) No net displacement of the beam centroid was observed. In fact, the instability had no discernable effect on the macroscopic parameters of the beam. One parameter that did evolve over the course of the simulation was the emittance, which grew as a result of imperfections in the initial match of the beam to the external fields. This growth was from $\epsilon_{n,rms} = 0.05$ cm-rad to 0.20 cm-rad. In an SST run with identical parameters, emittance grew from $\epsilon_{n,rms} = 0.05$ cm-rad to 0.13 cm-rad. It is not clear whether the difference in emittance growth between the ELBA and SST runs is caused by the instability or by differing particle statistics between the two codes. The latter is likely, however, as the final emittance in the SST code was reduced somewhat (< 10 %) when the number of particles was doubled.

Results for all runs are summarized in Table II. Growth rates and frequencies were

determined as described above for the $B_q k_q = 1000$ G/cm, $r_g = 3.0$ cm case, with theoretical values being taken from numerical solutions of Eq. (23) of Ref. 5. The two runs at $B_q k_q = 200$ G/cm showed growth rates that were too small to measure reliably. The $B_q k_q = 1000$ G/cm, $r_g = 4.0$ cm case, run D, was interesting in that the peak frequency of the TE_{11} mode spectrum clearly jumped between the primary instability at $\omega/c = 0.50 \pm 0.03$ cm^{-1}, and a higher frequency $\omega/c = 0.64 \pm 0.02$ cm^{-1}. The value listed in Table II for this case, $\omega/c = 0.54 \pm 0.07$ cm^{-1}, reflects a weighted average of these two frequencies. The higher frequency appears to correspond to the secondary mode at $\omega/c = 0.67$ cm^{-1}. From numerical solutions of the dispersion relation, the secondary mode should have a growth rate $\Gamma/c < 0.002$ cm^{-1} and, therefore, was not expected to play a role in these simulations.

III. Conclusions

An electromagnetic instability on an intense beam in a FODO lattice was studied via numerical simulation. We found evidence of the instability, with growth rates and frequencies in reasonable agreement with theory. The instability, however, was found to saturate at a low level, with field amplitudes two orders of magnitude lower than those observed in the helical quadrupole case. It had no discernable effect on the macroscopic properties of the beam.

This result is in sharp contrast to the corresponding instability in helical quadrupole fields. With helical quadrupole fields, the instability has been observed in simulations[1,3] and in experiments[4] to be extremely disruptive to beam transport.

We also find that the instability is broad-band in both frequency and wave number. We speculate that significant mode competition is occurring both among the various unstable wave numbers of the primary instability and, possibly, between the primary instability and the higher frequency secondary instability. It appears that the secondary instability may play a role in the growth of the primary instability despite the fact that its theoretical growth rate is more than an order of magnitude below that of the primary instability.

Acknowledgments

We would like to thank T. P. Hughes and D. Chernin for helpful discussions. This work was supported by the Defense Advanced Research Projects Agency, Arpa Order No. 7781, the Strategic Defense Initiative Organization/Innovative Science and Technology Office, and the Office of Naval Research.

References

1. T. P. Hughes and B. B. Godfrey, Phys. Fluids **29**, 1698 (1986).
2. C. M. Tang, P. Sprangle, J. Krall, P. Serafim and F. Mako, Part. Accel., **35**, 101 (1991).
3. J. Krall, C. M. Tang, G. Joyce and P. Sprangle, Phys. Fluids B **3**, 204 (1991).
4. M. G. Tiefenback, S. D. Putnam, V. L. Bailey, Jr., J. P. Lidestri and J. A. Edighoffer, Pulse Sciences, Inc. Report PSIFR-2543-01 (1991); T. P. Hughes, T. C. Genomi, K. Nguyen and D. Welch, Mission Research Corp. Report MRC/ABQ-OR-1442 (1991).
5. C. M. Tang, J. Krall and T. Swyden, to appear in Phys. Rev. A (1991).
6. T. P. Hughes and D. Chernin, submitted to Particle Accelerators.
7. G. Joyce, J. Krall and S. Slinker, in Proceedings of the Conference on Computer Codes and the Linear Accelerator Community, LANL Report LA-11857-C, 99 (1990).
8. D. Chernin, Part. Accel. 24, 29 (1988).
9. S. Humphries, Charged Particle Beams, (J. Wiley, New York, 1990), Chap. 4.
10. J. Krall, G. Joyce and S. Slinker, in Proceedings of the 14th International Conference on the Numerical Simulation of Plasmas, Annapolis, MD, 1991 (unpublished).
11. S. Slinker, G. Joyce, J. Krall and M. Lampe, submitted to Phys. Fluids B.

Table I

Run	I_b (kA)	$k_q B_q$ (G/cm)	k_q (cm^{-1})	r_g (cm)
A	1.0	200.	0.60	3.0
B	1.0	200.	0.40	3.0
C	2.0	1000.	0.55	3.0
D	2.0	1000.	0.55	4.0

Simulation parameters. Other beam parameters were $\gamma = 7$ and $\epsilon_{n,rms} = 0.16$ cm-rad for the $I_b = 1$ kA cases and $\epsilon_{n,rms} = 0.05$ cm-rad for the $I_b = 2$ kA cases.

Table II

	THEORY		SIMULATION	
Run	Γ/c	ω/c	Γ/c	ω/c
A	0.0057	0.62 ± 0.01	–	0.63 ± 0.03
B	0.0069	0.71 ± 0.02	–	0.55 ± 0.07
C	0.024	0.67 ± 0.03	0.023	0.58 ± 0.12
D	0.021	0.50 ± 0.01	0.027	0.54 ± 0.07

Theoretical values of peak linear growth rate Γ/c and frequency ω/c and corresponding simulation results. Simulation growth rates for runs A and B could not be determined reliably because the TE_{11} mode was largely masked by particle "noise" in those cases. Growth rates and frequencies are in units of cm^{-1}.

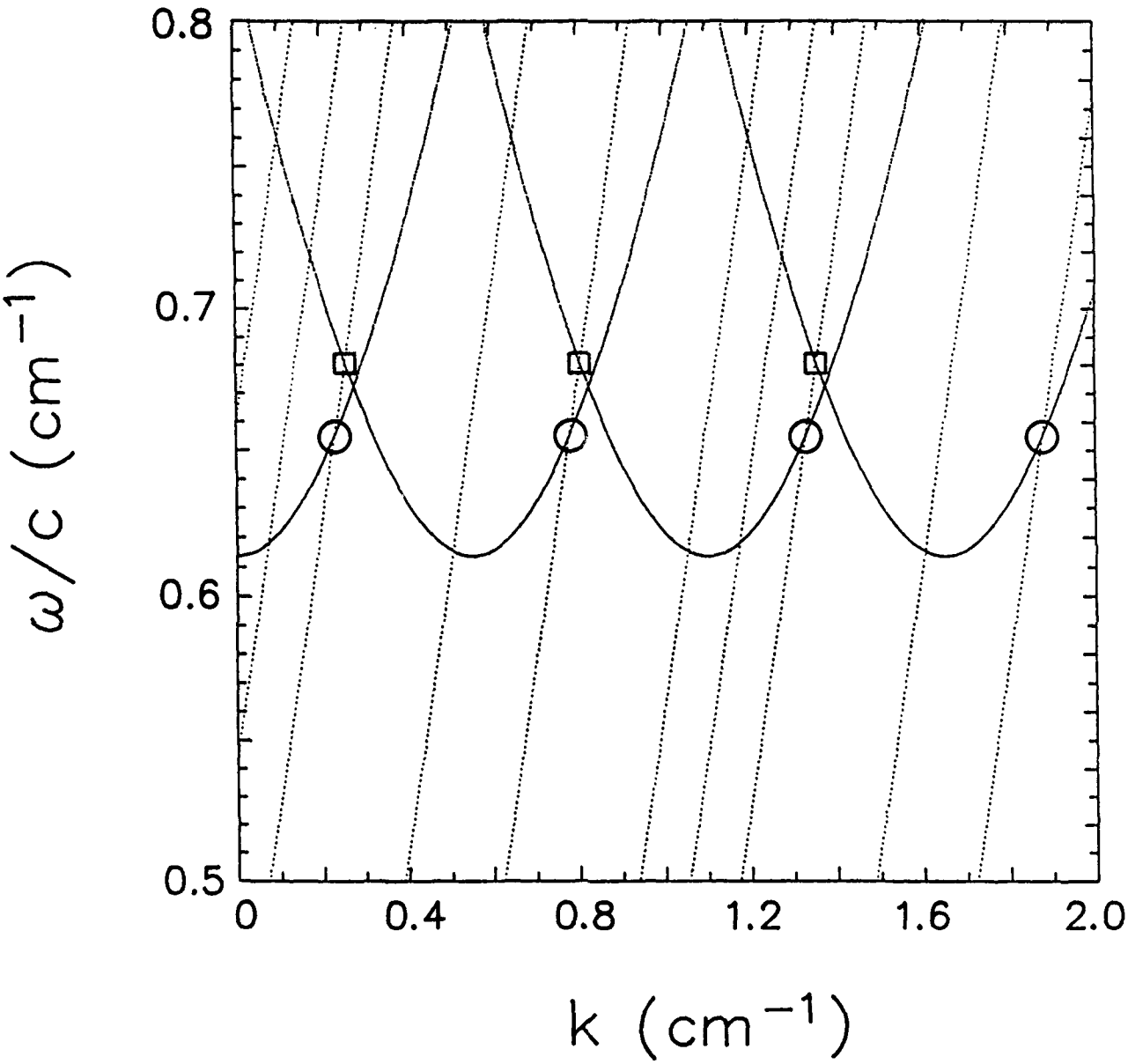

Fig. 1. Dispersion diagram in the low current limit. The primary instability occurs at points indicated by circles. A secondary instability occurs at points indicated by squares.

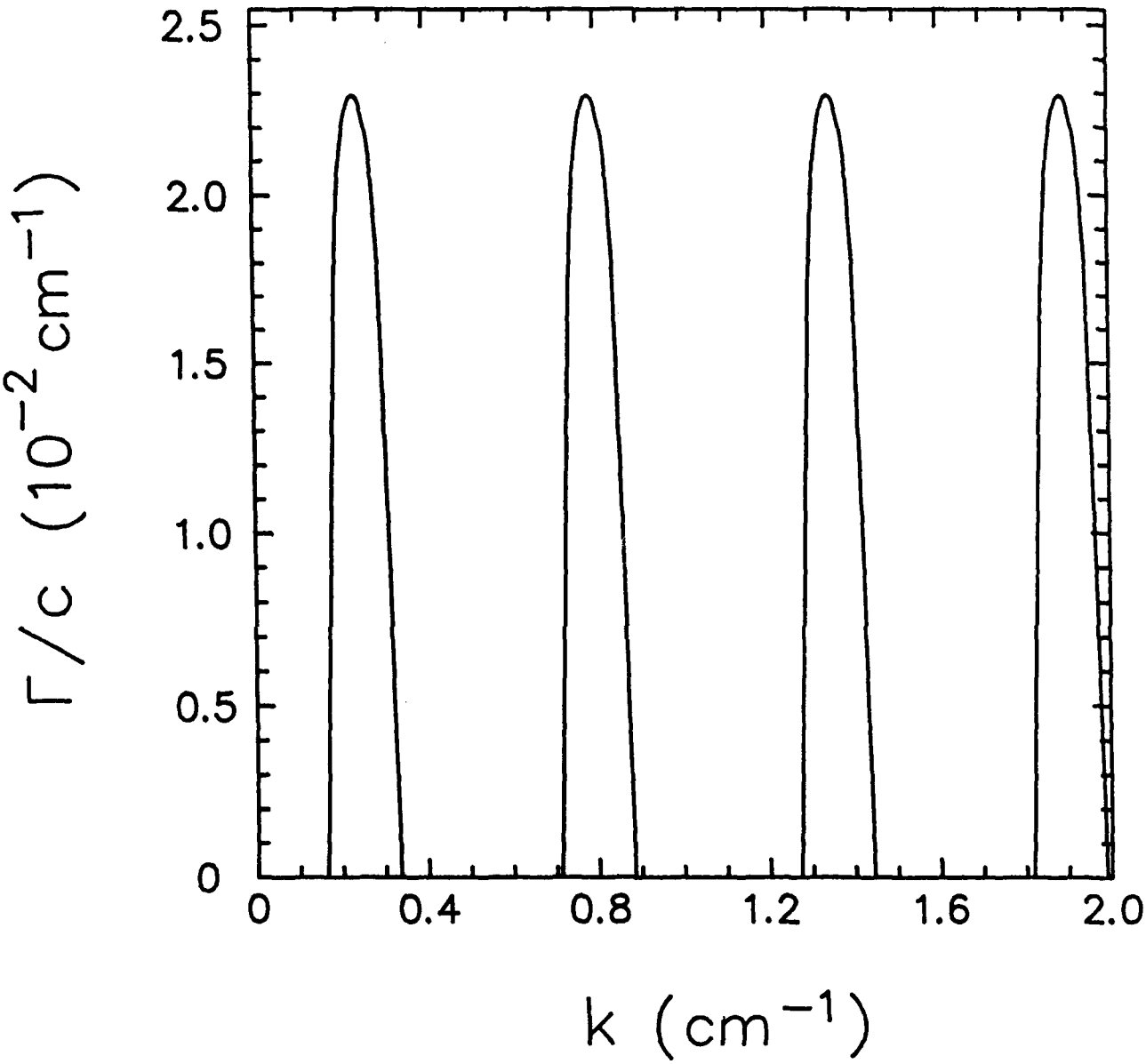

Fig. 2. Temporal growth rate of the primary mode for $\omega > 0$ as a function of wave number k for parameters listed in Table I, Case C.

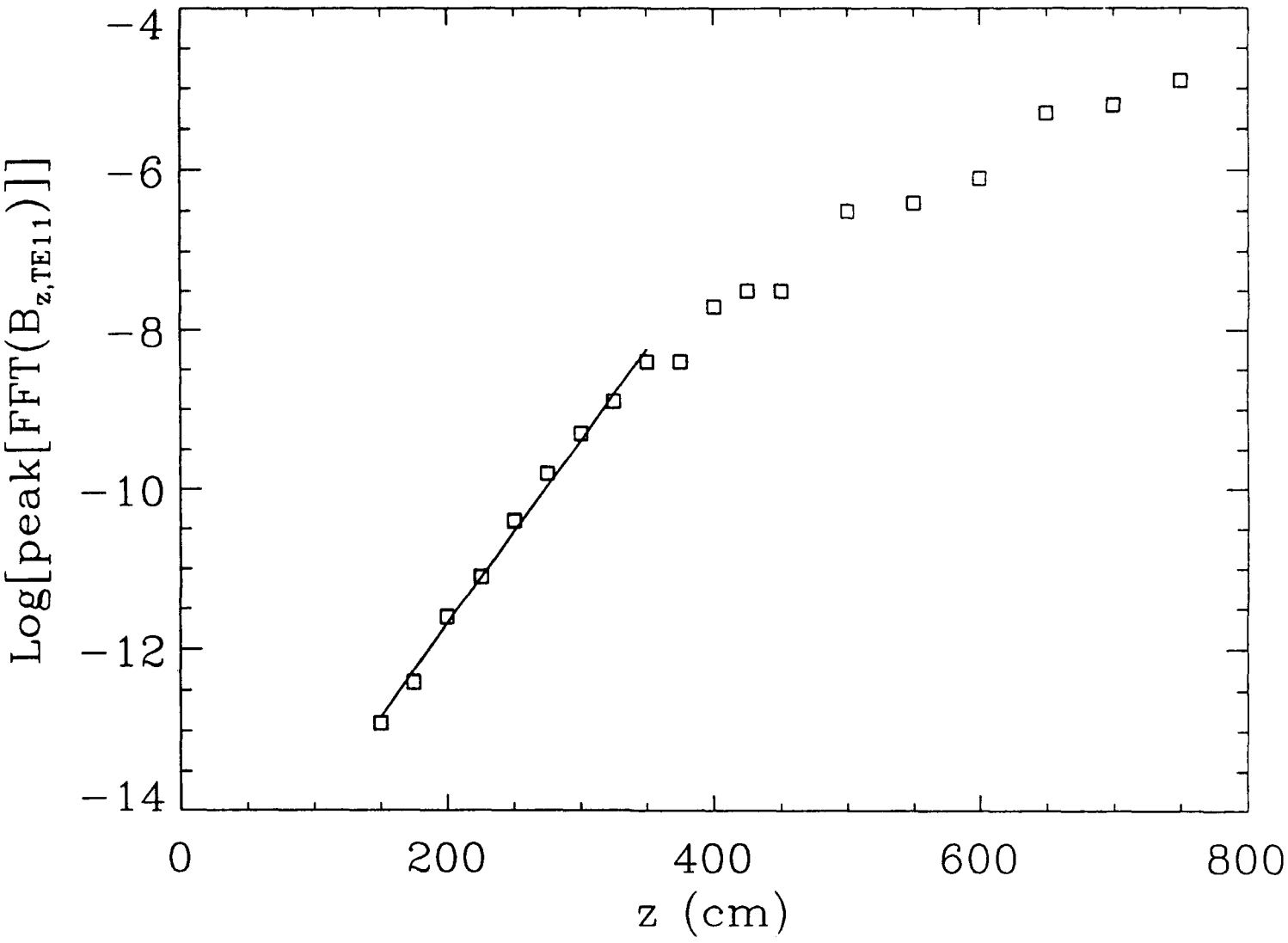

Fig. 3. The log of the peak of the Fourier transform, in frequency space, of the B_z component of the TE_{11} mode versus propagation distance for the $B_q k_q = 1000$ G/cm, $r_g = 3.0$ cm case (Case C in Tables I and II). A linear least-squares fit to the first nine points is also plotted.

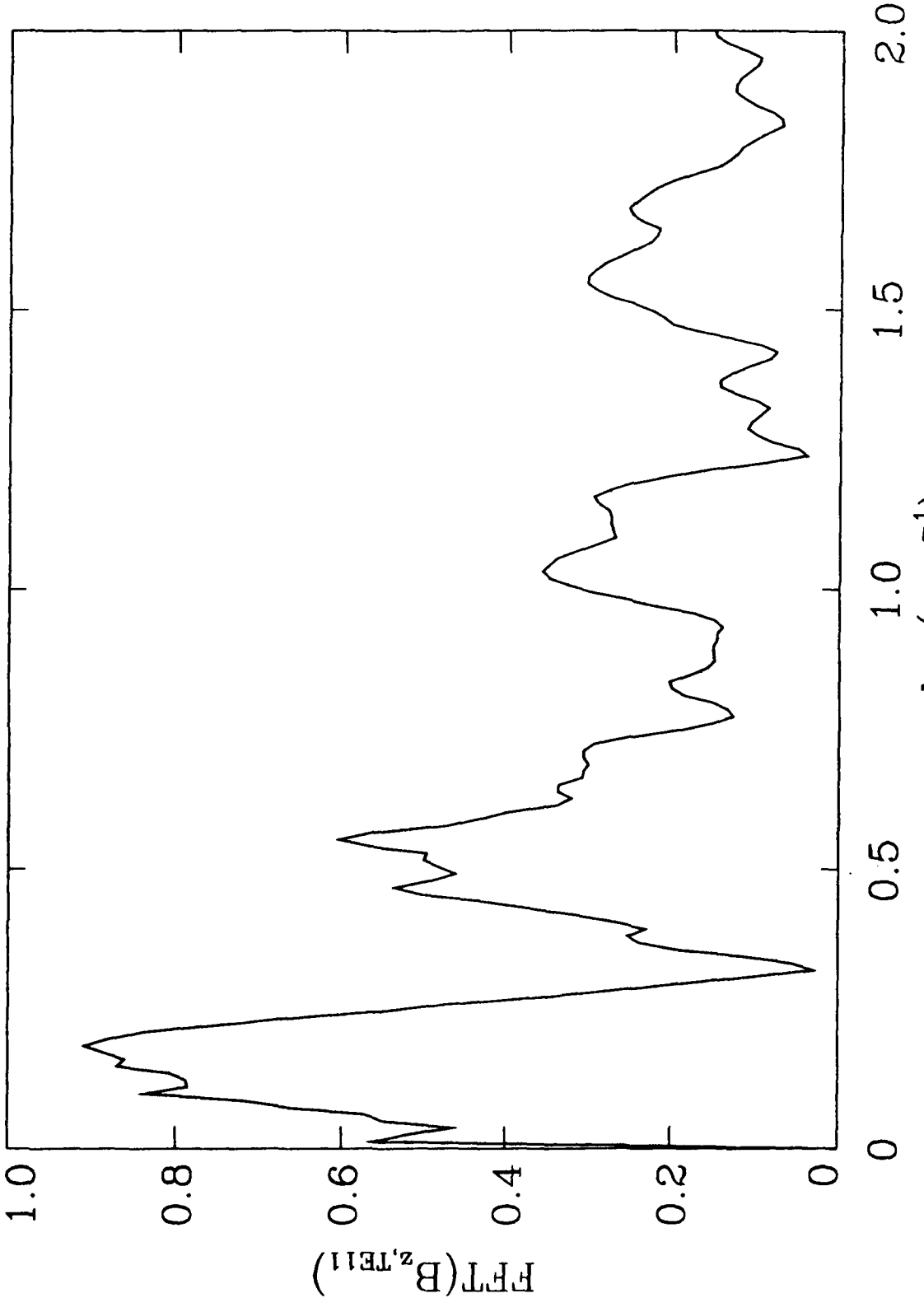

Fig. 4. Wave number spectrum at $ct = 175$ cm.

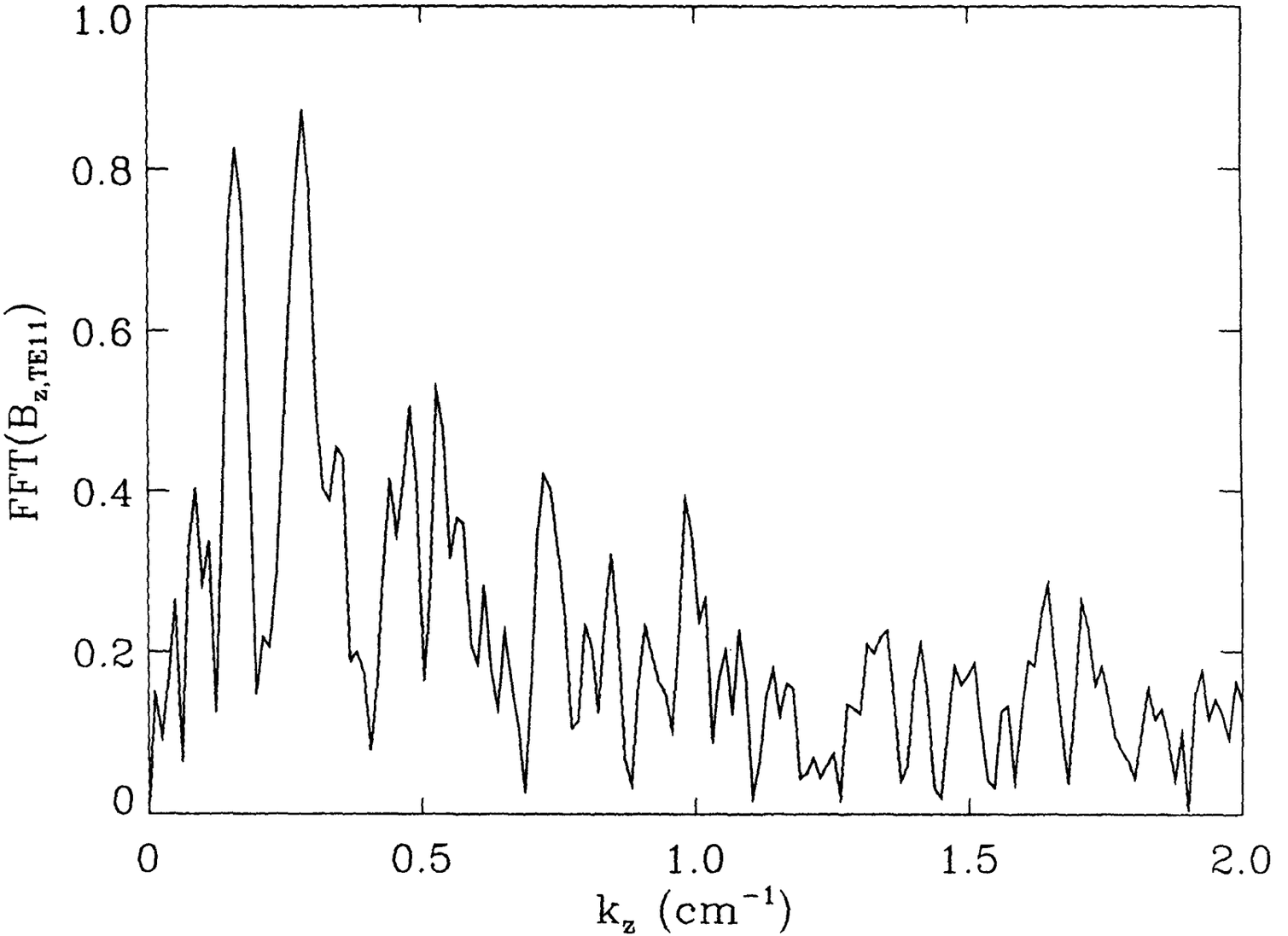

Fig. 5. Wave number spectrum at $ct = 1000$ cm.